

THE MASSES OF COOL SUPERGIANTS: THE INTERACTING ECLIPSING SYSTEM AZ CASSIOPEIAE*

A. P. COWLEY,†° J. B. HUTCHINGS

Dominion Astrophysical Observatory, Victoria, B.C., Canada

AND

D. M. POPPER

Department of Astronomy, University of California, Los Angeles

Received 1977 August 5

Data are presented from 63 spectrograms covering two cycles of the nine-year eclipsing system AZ Cas. The orbital elements are derived and it is seen that mass is lost from the M supergiant primary at periastron passage in an eccentric ($e = 0.55$) orbit. Several arguments suggest masses of ~ 13 and $18 M_{\odot}$ for the B and M stars, respectively. Spectroscopic phenomena are discussed which indicate the complexity of the mass flows in the system. Difficulties in interpretation of some of the observations remain. A short discussion is given of the observed masses of cool supergiants.

Key words: binaries, spectroscopic—binaries, eclipsing—mass exchange—massive stars

I. Introduction

AZ Cassiopeiae is one of a handful of known cool supergiants with a hot companion. Examples are the visual binary Antares, α Scorpii, and the spectroscopic binary, VV Cephei. In most cases we detect these systems as spectroscopic binaries because of the obvious composite nature of the spectrum (a blue continuum in the UV superimposed on an M supergiant spectrum at longer wavelengths (see review of these systems—Cowley 1969). Were it not for the great color difference of the two stars, the probability of recognizing them as binaries would be greatly diminished, as the orbital periods are very long (~ 10 years or longer) and the velocity amplitudes are small. In fact we do not yet know of any systems still on or near the main sequence with comparable periods and masses, presumably because of the difficulty in detecting such systems.

These stars are important to our understanding of evolution of massive stars because (1) they should provide a direct method of measuring masses of late-type supergiants and (2) they are the most luminous cool stars we know, and should provide information about mass loss of stars evolving from the upper main sequence. Because the separation of the stars is large, it can safely be assumed that until relatively recently the components evolved as single stars, only becoming

semidetached after the primary reached its present evolutionary state. The large orbital eccentricities (see Table VII) tend to confirm the suggestion that there has been little interaction in the past between the stars.

In this paper we shall present what evidence we can on the orbital parameters, masses, and model for AZ Cas and shall summarize the masses determined for other cool supergiants. We conclude that if these stars came from a representative sample of the upper main sequence, some of the primaries have lost a considerable amount of mass.

II. AZ Cassiopeiae

This system contains an M0 Ib (Bidelman 1969) and a hot B star whose H and He I lines are visible in the near UV, with approximately equal contributions near H γ . The system was found to be eclipsing by Ashbrook (1956) with a period of 9.3 years (3406 days). Very little photometric data and even less on the spectrum has been published, partially because the system is not bright ($m_v \sim 9.2$). No formal determination of the orbital parameters has previously been made, although in principle the system should yield a rather complete set of physical parameters (masses, radii, inclination, etc.) since it is both a double-lined spectroscopic binary and an eclipsing system. Furthermore the period is relatively short compared to other VV Cephei type stars, whose periods are all longer than 20 years.

III. Light Curve

Ashbrook's period of 3406^d was based on Harvard patrol plates between 1901 and 1948 and fits those

*Contributions from the Dominion Astrophysical Observatory, No. 347, NRC No. 16106.

†Visiting Astronomer, Kitt Peak National Observatory, which is operated by the Association of Universities for Research in Astronomy, Inc., under contract No. AST 74-04129 with the National Science Foundation.

°On leave from the University of Michigan.

data well. More recently Herczeg and Bonnell (1976) have discussed the period and suggested that 3402^d may be a better value. However, their period predicted a time of egress for the recent minimum in 1975 ten days earlier than it occurred. From an analysis of Ashbrook's data plus the information available for the 1957 and 1975 eclipses we find the orbital period lies between the above two values with

$$\text{JD min} = 2432481 + 3404(\pm 1^d)E$$

(Cowley and Hutchings 1977). We note that since our spectroscopic data only cover two cycles they do not allow formal improvement of this number. An uncertainty in the period of a few days does not affect the results we present here on the system parameters in any way. It does, of course, affect any discussion on the times of eclipse, particularly in the partial phases.

Some photoelectric photometry is available in the literature from the 1957 and 1975 eclipses. Larsson-Leander (1959) has covered part of the minimum and egress of the 1957 eclipse; photometry by Tempesti (1975) and Florkowski (1975) define well the 1st, 2nd, and 4th contacts and depth of minimum in several colors. Some of these data are shown schematically in Figure 1. We show the mean light curve derived from Ashbrook's data for the 1901–48 period (Ashbrook 1977) plotted on $P = 3404^d$. The duration of minimum light is $\sim 86^d \pm 3$. From a combination of data presented by Herczeg and Larsson-Leander, it seems likely that the 1957 eclipse had a longer duration than the mean eclipse given by Ashbrook. Spectra taken by Sahade (Méndez, Münch, and Sahade 1975) showing the partial eclipse phase, confirm the approximate time of ingress dotted in the diagram. Thus the duration of that minimum is clearly longer ($\sim 95^d$) than Ashbrook's value. Finally, since the most recent eclipse is quite well covered both photoelectrically and by some spectra, we know the totality lasted at least 105^d . Two possible interpretations are: (1) A real variation in the radius of the M star has occurred which would correspond to about a 5% change in the radius for the value of the inclination ($i \sim 80^\circ$) which we derive. This might be detectable as a change of magnitude of about $0^m.1$ over the last 25–30 years. (2) Alternatively, the highly interacting nature of the stars during the periastron passage ($e = 0.55$) may give rise to an apsidal motion. Given the present orientation of the orbit, one expects the duration of eclipse would increase. It is unclear what interpretation should be placed on the change of the eclipse duration, but the effect is too large to be due to observational uncertainty. We note that small changes ($< 1^d$) in the duration of totality are observed in similar systems such as ζ Aurigae and 31 Cygni. These variations have been interpreted as either changes in the radius of the primary or the opa-

city of the inner chromosphere. In 32 Cygni the variation is larger because the eclipse is grazing so that a small change in the effective radius can substantially alter the duration of the minimum (Wright private communication). Ashbrook's data do not indicate that this change in eclipse duration occurred prior to 1947.

IV. Spectroscopic Data

Because of the long period, spectrograms have been gathered from a number of sources: Hale Observatory coude plates taken by Sahade (see Méndez et al. 1975) in 1956–57 cover both the blue and red regions at 18 \AA and 26 \AA mm^{-1} , respectively. A series of red coude plates at 26 \AA mm^{-1} and Cassegrain spectrograph plates (39 \AA mm^{-1} in the blue) were secured by A.P.C. at KPNO with the 84-inch (2.1-m) telescope covering the period 1969–73. Since 1975, both red and blue plates, mostly at 40 \AA mm^{-1} have been taken at the DAO by J.B.H. and A.P.C. using both the 48-inch (1.2-m) and 72-inch (1.8-m) telescopes. A uniform series of blue plates at 45 \AA mm^{-1} have been taken at the Lick Observatory by D.M.P. covering the period 1966–76. These observations are listed in Tables I and II.

V. Velocities

The available plate material listed in Tables I and II has been measured at the DAO and UCLA, respectively. The DAO velocities are generally derived from at least 20 lines per plate, using rest wavelengths for the M star, β Pegasi (Davis 1947). Because of the variety of dispersions and spectral regions covered, it has been difficult to establish a uniform set of velocities among these plates. Two things are noticeable about the M star velocities: (1) the red-plate velocities are systematically more positive than the blue and (2) the blue plates individually show a greater spread in velocities. The latter point may be ascribable, in part, to blending difficulties in the blue region, although this spread shows some phase dependence, which is curious. We investigated the velocity-excitation dependence on all plates, thinking in terms of temperature gradients over a tidally distorted star of dimensions comparable with its orbit. Such effects were always small in the red region, but sometimes significant in the blue. The red region contains very few zero excitation lines, so that the effect is necessarily smaller at longer wavelengths. The blue region showed that the zero excitation lines agreed well with the red region velocities, and the excited lines showed a larger amplitude, and on the plates in hand had a maximum excursion near $0^{\circ}.6$, although our phase coverage is poor and this effect may not be, in fact, related to the orbital cycle. The UCLA data are intrinsically more noisy and we were unable to see these effects in them. However, they show the

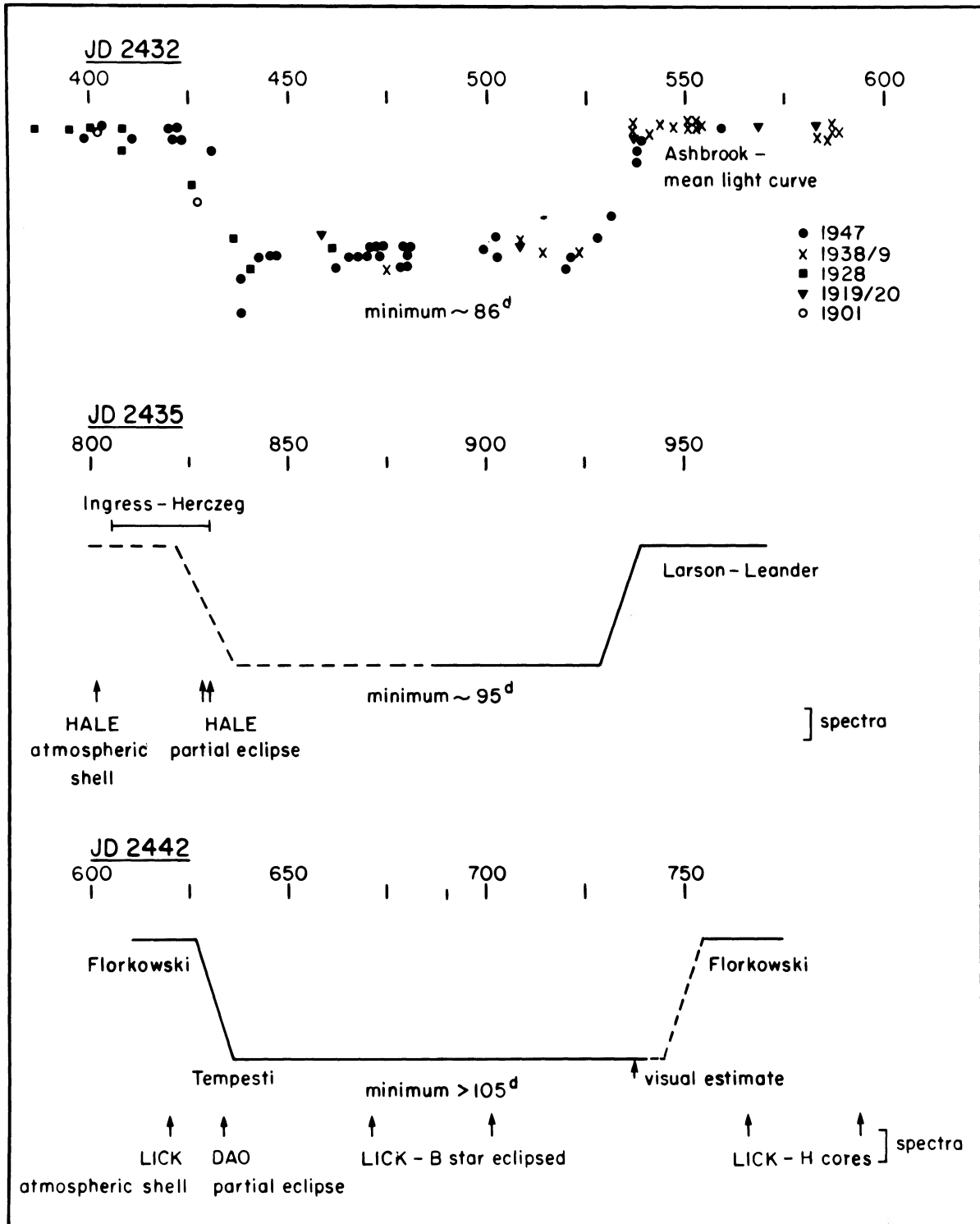


FIG. 1—Light curves for AZ Cas. Top panel shows Ashbrook's (1956, 1977) magnitude estimates from Harvard plates for five eclipses between 1901 and 1948. The vertical scale is arbitrary. The points have been phased with $P = 3404^d$. The JDs refer to the 1946 eclipse. The middle panel shows a schematic representation of the 1957–58 eclipse. The solid portion was covered photoelectrically by Larson-Leander (1959). Herczeg and Bonnell (1976) place the ingress in the range shown. Spectra confirm the B star was partially eclipsed during this time. The bottom panel shows the 1975 eclipse. The times of 1st and 4th contacts were observed photoelectrically by Florkowski (1975) who also gives the eclipse depths as $\Delta U = 1^m.77$, $\Delta B = 0^m.68$, $\Delta V = 0^m.25$, and $\Delta R = 0^m.19$. The time of second contact is from Tempesti (1975). Available spectra confirm the partial phases. The visual estimate made at the DAO shows the 3rd contact occurred after the time predicted by Herczeg and Bonnell (1976).

THE MASS OF AZ CASSIOPEIAE

885

TABLE I
Velocities from Hale, Kitt Peak, and DAO

JD 2400000+	phot phase*	dispersion/obs. (\AA mm^{-1})	M Star (km s^{-1})				CaII-K	em.	H α abs.	H (δ + higher)	3819 HeI
			low exc	high exc	mean (no.lines)						
35801.67	.976	18 B Mt. W.	-28	-22	-23.3 \pm 1.5(37)	-31	-	-	-21(1)	-	
35827.64	.984	18 B Mt. W.			-22.0 \pm 1.2(29)	-33	-	-	B star eclipsed		
35827.74	.984	26 R Mt. W.	-24	-28	-25.8 \pm 1.6(21)	-	+34	-63	-		
35830.84	.985	26 R Mt. W.			-30.1 \pm 0.9(25)	-	+10	-71	-		
36086.87	.060	18 B Mt. W.			-5.0 \pm 1.5(15)	-	-	-	-		
36117.79	.069	18 B Mt. W.	0	-4	-1.2 \pm 1.0(32)	-21(+34E)	-	-	-54(3)+14E		
36118.90	.069	18 B Mt. W.	-2	-7	-3.2 \pm 1.8(25)	-16(+55E)	-	-	-50(2)+20E		
40104.95	.240	40 IR KPNO			-39.5 \pm 2.5(10) [†]	-	-	-	-		
40489.98	.354	26 R KPNO			-43.0 \pm 0.8(30)	-	+33	-66	-		
40492.88	.354	26 R KPNO			-43.5 \pm 0.9(24)	-	+22	-75	-		
40869.84	.465	26 R KPNO			-45.1 \pm 0.6(24)	-	+21	-80	-		
40870.77	.465	26 R KPNO	-42	-44	-44.3 \pm 0.7(27)	-	+27	-76	-		
40871.84	.466	26 R KPNO			-41.9 \pm 0.6(30)	-	+24	-80	-		
41230.96	.571	26 R KPNO	-46	-43	-43.6 \pm 0.8(27)	-	+21	-74	-		
41231.86	.571	39 B KPNO	-49	-63	-56 \pm 2.1(17)	-23	-	-	-55(6)	-23	
41231.93	.571	39 B KPNO			-59 \pm 2.8(15)	-32	-	-	-81(6)**wing	-57	
41614.65	.684	39 B KPNO	-38	-49	-49 \pm 3.3(6)	-34	-	-	-33(3)	-65	
41616.74	.684	39 B KPNO	-58	-66	-61 \pm 3.1(14)	-16	-	-	+4:(4)	-2	
41618.87	.685	26 R KPNO			-45.0 \pm 0.8(27)	-	+24	-78	-		
42003.56	.798	78 B KPNO			-52.1 \pm 3.0 (16)	-28	-	-	-62(8)	-66	
42004.56	.798	39 B KPNO			-34.7 \pm 3.5(8)	-26	-	-	-64(3)**	-	
42004.59	.798	39 B KPNO			-38.1 \pm 30(11)	-24	-	-	-62(6)	16	
42004.63	.798	39 B KPNO	-33	-49	-42.5 \pm 3.2(14)	-15	-	-	-48(7)	55	
42008.81	.799	25 R KPNO	-41	-39	-38.8 \pm 0.9(19)	-	+27	-72	-		
42633.93	.983	40 B DAO			-29.9 \pm 1.1(25)	-61	-	-	B star eclipsed		
43081.84	.115	40 B DAO	-10	+3	-1.6 \pm 1.8(43)	-	-	-	-		
43165.79	.139	31 B DAO	-8	-1	-2.0 \pm 2.0(44)	-	-	-	-		
43239.88	.161	40 B DAO			-33.3 \pm 2.2(27)	**	-	-	+1(5)core**	18	
43261.80	.167	40 R DAO			-21.9 \pm 1.3(31)	-	-27 base +11 peak	-	-		

*T = 2432481; P = 3404^d[†]from R. Humphreys (private communication)

**emission complicates these lines

same velocity variation as our red and zero-excitation blue data. In the absence of any adequate explanation, we have omitted the blue excited (2-4 eV) line velocities from the orbital solution, wherever they are significantly different from the mean (see Table I). However, in Table I we present velocities for both high- and low-excitation lines as well as the mean value.

The Lick velocities of the M star, given in Table II, are derived from a list of 12 lines in the region

$\lambda\lambda 4063-4405$ on the same wavelength system used for velocities in Table I from plates in the blue region. The Lick velocities are systematically more negative at corresponding dates than those of Table I by 3 km s^{-1} . The internal mean error of a plate is 6 km s^{-1} . It was felt that this difference was not significant, and it makes almost no difference to the derived orbital parameters.

In the Lick velocities a systematic change of about 8 km s^{-1} is suggested between cycles, in the overlap re-

TABLE II
Velocities and Line Strengths from Lick Plates

JD 2400000+	Phot Phase*	M Star [†]	H	λ 3819 HeI	CaII-K	[FeI] **	Hydrogen Emission or Absorption Core	H β + γ [‡] Absorption Strength	Remarks
39399.812	.033	-34	-	-	-34	+ 4	-43 core	5.8	
426.837	.041	-26	-	-	-22	0		6.5	
427.765	.042	-26	-	-31	-15	+ 3	-29 core	4.5	
482.619	.058	-27	-	-	-	-		-	(weak)
719.987	.127	-28	-45	-18	-	+16	-51 em	em	
757.966	.139	-28	-	-	-	+ 9	-34 em	em	
783.857	.146	-45	-85:	-45	-	+ 4	-36 em	em	
40105.935	.241	-38	-34	0	-13	- 6		0.8	
170.853	.260	-44	-	-36	-21	+ 5		1.2	
227.776	.277	-39	-	-	-15	- 1		1.1	
459.989	.345	-38	-55	-24	-12	-10		2.2	
520.754	.363	-47	-59	-60	-26	-18		3.7	
545.722	.370	-49	-52	-23	-19	-22		2.5	
877.825	.467	-48	-	-	-	-19		3.8	weak plate
933.649	.484	-43	-57	-42	-22	-19		2.8	
41199.923	.562	-43	-62	-29	-21	-35		2.7	
557.969	.667	-48	-63:	-50	-22	-21:		3.8	
614.836	.684	-43	-60	-43	-38	-32:		4.5	
905.963	.769	-52	-75	-	-31	-37		4:	
941.907	.780	-49	-71	-	-30	-31:		3.2	
42024.646	.804	-47	-81:	-19	-38	-34:		3:	
087.635	.823	-44	-69:	-	-20	- 7		4.5	
292.907	.883	-42	-91	-55	-37	-22		6	
374.880	.907	-39	-54	+20	-29	-11		6.5	
437.643	.925	-29	-68	-70	-17	-20	-16: core	6	
42619.974	.979	-35	-59:	-	-28	-18	-26: core	5.8	
671.968	.994	-18	-	-	-	-15		1.1	eclipse
702.863	.003	-26	-	-	-	- 6		1.0	eclipse
765.656	.022	-25	-85:	-	-45	-14	-44 core	5.8	
794.616	.030	- 8	-70:	-51	-37	- 8	-38 core	6.5	
43060.795	.108	-17	-91	-82	-49 em	+ 5	-39 em	em	
120.712	.126	-18	-	-46	-	-23	-49 em	em	
178.680	.143	-31	-	-	-	0:		wk em	(weak plate)

*phase from JD 2432481 + 3404 E

†mean error $\pm 6 \text{ km s}^{-1}$ **using rest wavelength λ 4243.98

‡eye estimate relative to neighboring late-type lines

gion 0^p0 to 0^p15. In this connection, we note that the Lick velocities prior to JD2440000 are systematically lower than any others at this phase. Since irregular variations, both in light and velocity, are common in cool supergiants differences from cycle to cycle are not unexpected. In the next section we discuss the consequences of assuming that these velocities may not be representative of the orbit, perhaps because of unusually strong blending of the atmospheric shell spectrum after periastron passage. D.M.P. has also noted during this period that the H emissions were stronger than on the most recent plate ($\phi = 0.14$) of the current cycle, indicating additional circumstellar material may have been present.

The H velocities in Tables I and II are from the broad Balmer lines in the B-star spectrum for H δ and higher H lines. He I λ 3819 was measured on most Lick plates and a number of others. Its appearance is variable, and the velocities are badly scattered. He I λ 4026 is badly blended with lines of the M star. Also included are velocities from the sharp Ca II K line and from hydrogen emission and sharp core absorption lines when these features appear most strongly.

Forbidden emission of [Fe II] at λ 4244 was measured on most of the Lick plates. Since its mean velocity, assuming a rest wavelength of λ 4243.98, lies about 30 km s⁻¹ higher than the stellar lines, we assume that the line is either a blend with another [Fe II] line at λ 4244.81 or its profile is distorted by nearby stellar absorption features.

VI. Orbital Elements and the Motion of the B Star

Orbital parameters have been computed for all of the data as well as various subsets. In all cases the period was fixed at $P = 3404^d$. In Table III we present the most relevant results. Use of Ashbrook's 3406^d period makes no difference to these values. Note that if the discrepant first seven Lick velocities are omitted, the DAO and Lick results give essentially the same elements. We adopt the solution with all data except for the early Lick velocities and the blue high-excitation lines, as discussed in the previous section. A correction to eliminate the 3 km s⁻¹ difference between DAO and Lick velocities makes a negligible difference to the elements, and was not applied. We note the extremely eccentric orbit, which will be shown to be closely connected with the spectral appearance. Because of this changing appearance, because of the inconsistent velocities at certain phases from cycle to cycle, and because atmospheric eclipse effects may distort the velocities near eclipse ($\phi_{\text{phot}} = 0.0 \pm 0.1$), these orbital parameters, in particular the high eccentricity, should be treated with caution. In what follows we implicitly assume, however, that the adopted orbit-

al elements represent the true motions of the stars. The reader should be aware that many of the conclusions of this paper are based on this assumption. In Figure 2 we show the velocity curve based on the adopted elements.

It is unfortunate that, according to the adopted elements, the orbit is oriented so that periastron passage ($\phi_{\text{phot}} = 0.08$) occurs shortly after eclipse of the B star, so that eclipse effects and periastron effects on the appearance of the spectrum overlap in time. On the other hand, velocities from the red spectral region should be unaffected, as we see no changes with phase in the appearance of the absorption spectrum in this region. Despite the limited phase coverage of the red velocities, their fit to our adopted orbit lends support to its reality. In contrast, the atmospheric eclipse and partial eclipse greatly alter the spectral appearance in the blue (see Fig. 5), even causing Mendéz et al. (1975) to compare the star to an F8 I star just before eclipse.

One very obvious effect, especially in the Lick material which has more uniform phase coverage, is the increased scatter in the velocities between $0 < \phi_{\text{phot}} < 0.2$, which is primarily due to a different average velocity between the two cycles covered by the Lick data. We attribute this to disturbances and changes which arise on the M star due to the close passage of the B-star companion which may vary from cycle to cycle. Other evidence that longer term variations in the spectrum exist is presented below. In Figure 3 we present a schematic diagram of the orbit (views both in the plane and from the pole) indicating the relative separations of the objects and their sizes based on a mass ratio $q \sim 1$. The M star is shown filling its "Roche lobe" at periastron passage.*

It was hoped that a definitive mass determination for both stars could be made using the B- and M-star velocities. We find that both the higher Balmer members and He I λ 3819 show a large scatter, and that the former have largely negative velocities (see Fig. 4). In the case of the H lines it is clear that near periastron they become partially filled with emission, so that their absorption-line velocities are very difficult to measure. It may be that the negative H velocities also reflect mass loss from the B star. This interpretation is offered by Mendéz et al. to account for the ~ -50 km s⁻¹ displacement on their plates, (which are the Hale plates also studied in this paper.) It is not clear if the He I λ 3819 velocities are also affected partially by emission. The individual velocities of this line show

*We are aware that the Roche geometry is not strictly applicable in a noncircular orbit, but in the absence of a rigorous treatment of the question, we believe it to be a good approximation in view of the long period of the orbit in comparison with the dynamical time scales of these stars.

TABLE III
Orbital Elements for AZ Cas from M Star Absorption Lines
P = 3404^d, fixed

Data	No. of obs.	V_0 (km s ⁻¹)	K (km s ⁻¹)	e	ω (°)	T (JD2400000+)
Lick	33	-40.0±1.2	12.8±1.6	.38±.11	-16±20	39386±141 ^d
Lick*	26	-38.4±1.1	21.3±4.5	.59±.09	- 3±8	39501±41
DAO†	30	-35.8±1.2	22.9±2.4	.55±.06	10±10	39596±56
All**	56	-36.6±0.8	22.1±1.7	.55±.04	4±7	39554±40
[Fe II]	31	-15.3±1.4	18.4±2.1	.25±.09	- 5±26	39779±219

*Lick data prior to JD 2440000 omitted.

†DAO means all spectra reduced in Victoria, and includes KPNO, Hale and DAO plates.

‡Adopted orbit. For these orbital elements we derive:

$$a_1 \sin i + 8.6 \times 10^3 \text{ km}$$

$$f (M) = 2.2 M_{\odot}$$

large scatter and we are unable to derive any value of the mass ratio from them, although we note that their mean value of $-31 \pm 6 \text{ km s}^{-1}$ is close enough to the adopted V_0 velocity of the system to expect that with higher-quality data in the UV it might be possible to determine a meaningful orbit for this star.

We have made eye estimates of the $H\beta$ and $H\gamma$ emission strengths to assess the effects of emission on the measured H-line velocities. We find two effects are present (see Fig. 4): (1) The emission is markedly strengthened at the time of periastron passage and decays slowly. Probably the M star overfills its inner Lagrangian surface (or the equivalent in a time variable frame) at that time and the material lost from the M star is seen in emission. (2) $H\beta$ emission is not seen during the eclipse, suggesting that it is formed in a more limited region than $H\alpha$, either between the stars or quite near the hot star.

The [Fe II] emission lines yield a marginally smaller semiamplitude, K , than was found for the M star, and a lower eccentricity (see Table III). The V_0 discrepancy is probably due to the uncertainty in rest wavelength (see previous section). The ω and T for [Fe II] suggest a possible phase lag (~ 0.06) with respect to the M star, although the uncertainty is large. In a schematic picture the material primarily leaves the M star near periastron passage. The [Fe II] lines may arise in a low-density region loosely associated with the M star, but trailing it and somewhat closer to the center of mass. Undoubtedly the extent and orientation of the region is variable with time. In two spec-

troscopically similar systems, VV Cep (Peery 1966) and HR 2902 (Cowley 1965), [Fe II] appears to be formed in an extended region surrounding both stars, and shows no orbital motion. These systems, however, are wider pairs, with periods of 21 and 27 years, respectively. We note that in the symbiotic binary AR Pavonis (Thackeray and Hutchings 1974), the forbidden emissions were found to be associated with the M star, although the details were different.

Other lines which were measured are given in Tables I and II. During most of the orbit the Ca II lines are present as strong, sharp absorptions with a mean velocity around -25 km s^{-1} . There seems to be a tendency for them to become slightly more negatively displaced as the orbital phase changes (~ -20 near $\phi = 0.3$ and ~ -30 near $\phi = 0.9$). Their origin would appear to be circumstellar, as they disappear near $\phi = 0.1$ and then go into emission as the H emission becomes strong. However, considering the distance of AZ Cas, it seems probable that part of the absorption must be interstellar. The maximum relative contribution from the interstellar component is presumably present when the hydrogen-core spectrum is weakest, near phase 0.25. We have compared the strength of the sharp K line in AZ Cas at this phase with its strength in the spectra of two stars nearby in the sky: HD 12509 (B1 III; $(m - M)_0 = 9.7$) and BD +60°343 (B2 II; $(m - M)_0 = 11.5$), where the spectral types and distance moduli are from Hiltner (1956). The K line in AZ Cas at these phases is intermediate in strength between the two comparison stars, implying

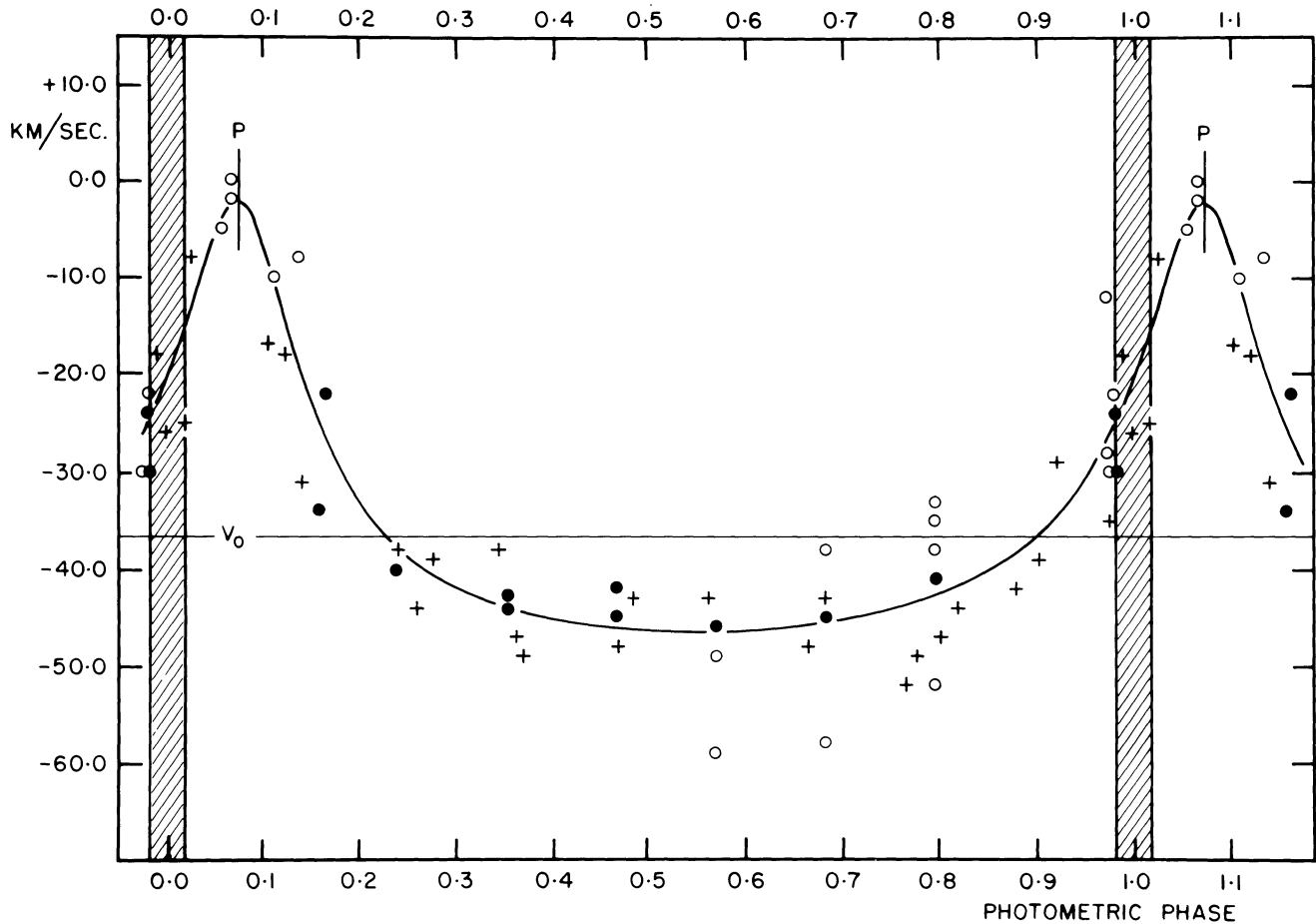


FIG. 2.—Observed velocities and adopted orbit for AZ Cas. The open and closed circles are blue and red plates, respectively, from Hale, KPNO, and DAO. The crosses are Lick velocities. The early Lick velocities and those from the high-excitation blue lines, not used in the adopted solution, are omitted. The time of totality is shown by the shaded portion of the figure. The time of periastron passage is marked by “p”. The corresponding orbital elements are given in Table III.

an interpolated distance modulus of no more than 10.5, allowing for a circumstellar contribution to the line. The correspondingly lower luminosities of the components of AZ Cas implied by the smaller distance modulus would remove the consistency of parameters (and evolutionary inferences) derived in the discussion in section IX. We conclude the true distance modulus must be much larger than is inferred from the K-line strength alone.

In Table II we give estimates on an arbitrary scale of the average on each Lick plate of the intensities of the sharp absorption lines at $H\beta$ and $H\gamma$ (except when emission is present) relative to neighboring absorption lines in the spectrum of the M star. At these wavelengths the spectrum of the M star dominates, and the intensities are essentially unaffected by broad underlying absorption from the B star. Near $\phi_{\text{phot}} = 0.25$ these lines are as weak as they are during total eclipse, and increase gradually in strength with advancing phase, reaching their maximum intensity just before

and just after eclipse, when these core lines of H extend to high Balmer series members. The velocities of the H core lines at these phases are also given in Table II. The variation in H-line absorption intensities is roughly correlated with the distance of the B star from the observer. Thus, if there is a large gaseous envelope surrounding the M star, absorption could occur when the B star is on the far side of its orbit. As the B star moves close to the M star near periastron, the material is ionized, giving rise to the observed emission lines.

VII. Stellar Parameters

Some rectified tracings are shown in Figure 5 and related measurements in Figure 6, which illustrate several points. As noted, the B-star spectrum shows considerable emission following periastron. At $H\beta$ and higher Balmer lines these changes do not appear more than ~ 0.1 before periastron and we regard this as strong evidence that mass transfer occurs as a result of the M star filling (or very nearly filling) its “Roche

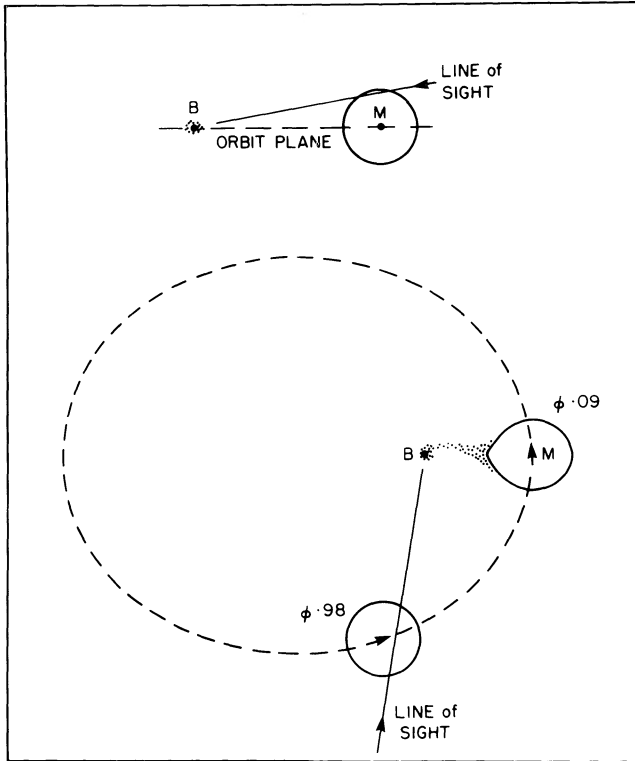


FIG. 3—Views in the orbital plane and from the pole of the AZ Cas system. The system apparently is viewed slightly out of the plane ($i \sim 80^\circ$). Because the orbit is highly eccentric ($e = 0.55$) the separation of the components changes by a large amount.

lobe” at periastron. A similar situation occurs in HD 187399 (Hutchings and Redman 1973), where $e \sim 0.4$. At $H\alpha$ the emission is also phase dependent, but the changes last longer (see Fig. 4).

The eclipses show an interesting consistency with the derived value of ω . From the shape of the velocity curve we know that the stellar velocity changes considerably through eclipse. The result is that transverse velocities of the components increase by a factor 1.7 between first and fourth contact. We estimate (see Fig. 1 upper panel) that the mean durations of ingress and egress differ by three days in the expected sense.

If we now assume: (1) the M star fills what would be its Roche lobe corresponding to periastron separation, (2) the orbital parameters in Table III, and (3) a mean eclipse duration (1st-3rd contact) of 100 days, we derive the values shown in Table IV for stellar radii, masses, and inclinations. Note that the inclination is fairly well defined (near 80°) and that the B-star radius (defined by the duration of ingress (or egress) of nine days and assuming a geometrical interpretation for the eclipse) is not a strong function of q . However, the values for this quantity are typical of a supergiant, and since we have reasons for concluding the hot star is on the main sequence (see below), we conclude that the

derived ‘radius’ includes the effects of an extended envelope around either star or both. Detailed photometry during the partial phases may help clarify this point. Note also that normally accepted values for M supergiant radii are in the range 600–700 R_\odot , which implies a preferred value $q \sim 1.4$. Below, we discuss further reasons for selecting this value of q .

VIII. The B Star

The absorption spectrum seen in the near UV roughly resembles a B0–1 star. It is hard to classify precisely as the M star obliterates the weak lines used in spectral classification. It is also possible that the spectrum changes with phase: the Balmer equivalent widths (EWs) and some He I lines appear to vary (see Figs. 5 and 6). Balmer emission is clearly present in many lines in phases following periastron (as has been noted) and the sharp Ca II lines are missing at this phase. A mean $H\gamma$ equivalent width out of eclipse (estimated from the more accurately measured H8 and H8 EWs) is $\sim 4.5 \text{ \AA}$. This corresponds to $M_v \sim -3$ or $M_{\text{BOL}} \sim -6$ in a normal star, which is just the luminosity of a main-sequence B0 star ($M \sim 15 M_\odot$). However, the radial velocity of the Balmer lines is generally shifted by $\sim 40 \text{ km s}^{-1}$ from the systemic velocity so that it is doubtful whether the spectrum is normal. The shift may be due to absorption by an expanding outer envelope or to filling in by red-shifted emission. Both possibilities may occur since (1) the B star will tend to lose mass from an accretion disk, like a Be star, and (2) the bulk of the mass loss from the M star occurs at periastron when half of the M star surface is moving away from us at velocities exceeding escape for the system. Thus, the B-star luminosity might be somewhat lower than is indicated above, although we argue below that this is unlikely.

The rotational velocity estimated from He I $\lambda\lambda 3819, 4026$ on several plates, is $\sim 300 \pm 20 \text{ km s}^{-1}$. If this is a rotational broadening, it is consistent with accretion of angular momentum from the matter transferred from the M star.

IX. The Masses and Luminosities

The cool star has been classified M0 Ib by Bidelman (1969), from spectra in eclipse, which implies a temperature of $\sim 3200 \text{ K}$. In Table V we show implied luminosities for temperatures near to this value, and radii corresponding to q values used in Table IV. We see that good agreement is obtained between masses corresponding to these values (Table IV) and those derived from evolutionary tracks on the H-R diagram, for q values near to 1.4.

Photometry of AZ Cas gives $m_V = 9.24$, $m_B = 11.0$ out of eclipse (Wawrukiewicz and Lee 1974), and m_V

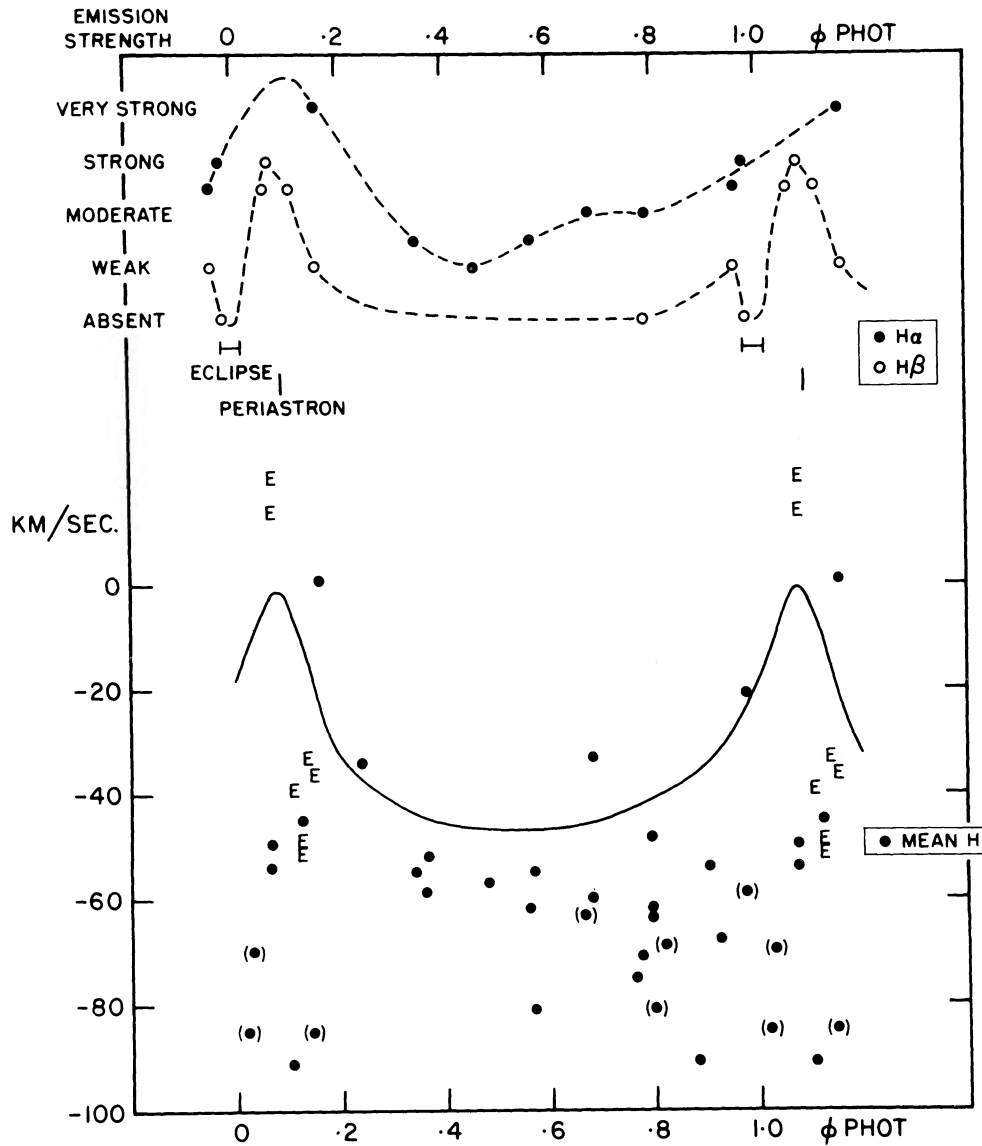


FIG. 4—(above) Eye estimates of the strength of H α and H β emission. (below) Velocities of the H absorption lines with phase. Values in parentheses are uncertain. E denotes the measured lines are in emission. The smooth curve represents the adopted orbit of the M star.

$= 9.5$, $m_B = 11.6$ (Tempesti 1975) in eclipse. These figures imply that $E_{B-V} \approx 0.6$, and that $m_V = 11.3$, $m_B = 11.6$ for the B star, with the same reddening. Our ratios of M to B star line depths (Fig. 6) confirm these figures in the B and U regions. If we take $M_V = -2.8$ for the B star, as discussed above, and $M_{BOL} = -6.5$ for the M star, from Table V, with $T \sim 3200$ K, we find (see Table VI) a consistent distance estimate for each star, of ~ 2.8 kpc. (This distance is close to the value adopted by Stothers (1972) for the association Cassopeia OB8, in the direction of which AZ Cas lies.) These luminosities place the B and M stars on the H-R diagram with main-sequence masses of $\sim 13 M_{\odot}$ and $18 M_{\odot}$, respectively, with the evolutionary tracks of Chiosi, Nasi, and Sreenivasan (1977). These values

agree very well with the masses given by the mass function for $q = 1.3$ or 1.4 . If the B-star luminosity is significantly lower than what we assume here, we cannot obtain this consistency in distance and mass estimates.

The evolutionary tracks of Chiosi et al. take into account mass loss by a single star, so that the M star of mass $\sim 18 M_{\odot}$ initially, may now be $\sim 15 M_{\odot}$. This is in accordance with known mass-loss mechanisms for massive stars. In this case, mass is being lost in the present state by Roche lobe overflow as well, and this could conceivably mean that the mass is underestimated from the H-R diagram. However, the mass-loss rate is not high compared with other evolutionary stages, and the general consistency of the above num-

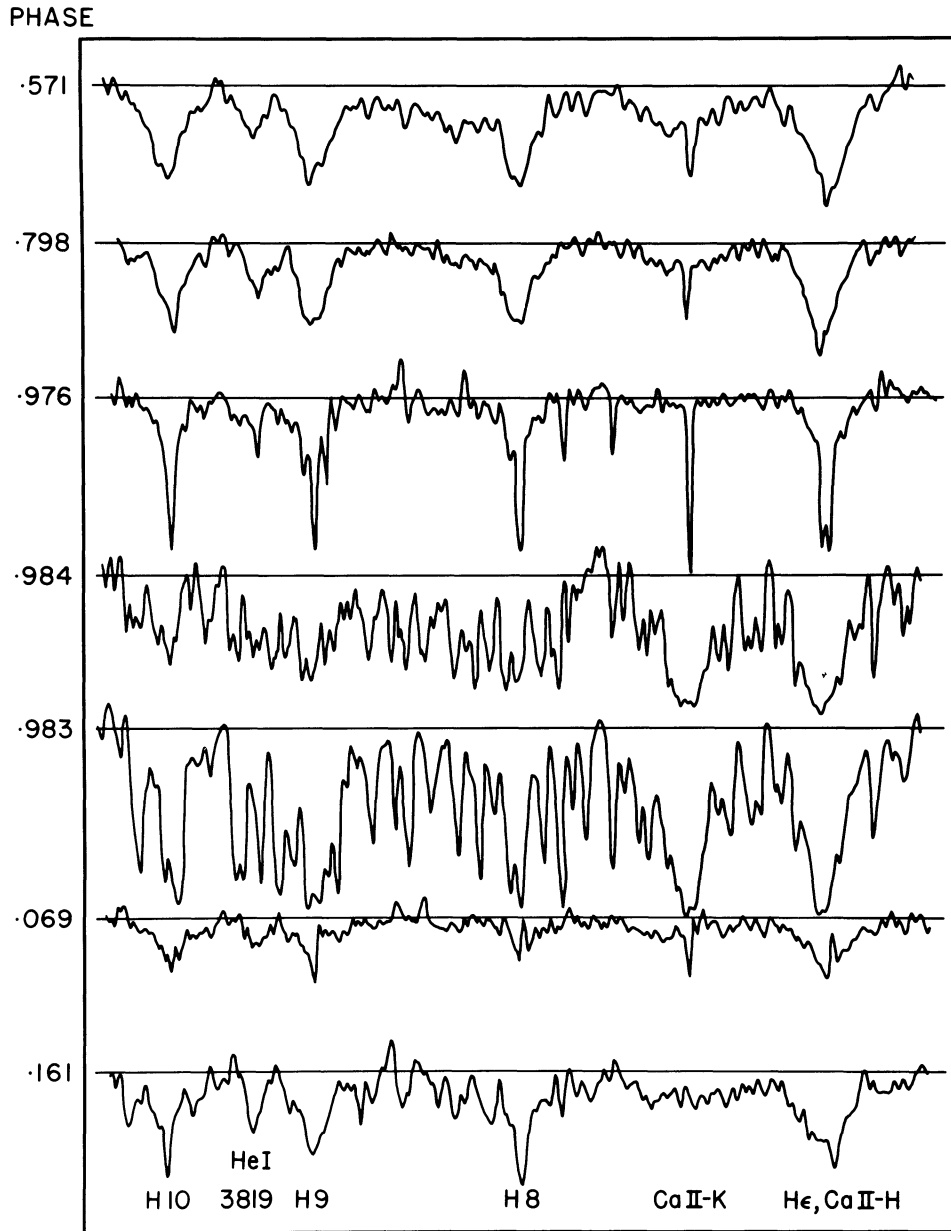


FIG. 5—Rectified intensity tracings of AZ Cas spectrograms from selected phases. The Julian Dates for each of the tracings are: $\phi = 0.571$, JD2441232; 0.798, JD2442005; 0.976, JD2435802; 0.984, JD2435828; 0.983, JD2442634; 0.069, JD2436119; and 0.161, JD2443240. In the upper two tracings, far from eclipse one sees the B star primarily in this region of the spectrum. At $\phi = 0.976$ the B star shines through the extended outer atmosphere of the M star and “shell” absorptions (cores) appear in the H and Ca II lines. Note the strong Ti II $\lambda\lambda 3900$ and 3913 lines, typical in such eclipsing systems. At phase ~ 0.98 the B star is nearly eclipsed and the broad Ca II lines of the late-type star predominate in this spectral region. Note that the two tracings at phase ~ 0.98 differ. In the 1957–58 eclipse (upper) more of the B-star continuum contributes to the spectrum than in the 1975 eclipse (lower). Either uncertainty of a few days in the period or change of eclipse duration could account for this difference. The plate at $\phi = 0.069$ was taken just prior to periastron passage. Note the slightly red-displaced emission in the H and Ca II lines. By $\phi = 0.161$ the emission in the higher Balmer lines is weaker and displaced to the violet side of the absorption. The Ca II K line appears to be totally filled by emission.

bers suggests that the binary mass transfer has not affected the evolution of the M star significantly yet.

X. Conclusions and Comments of the Masses of Late-Type Supergiants

We suggest that the system AZ Cas consists of a B0

main-sequence star and an M0 supergiant in an eccentric orbit in which the M star fills (or overfills) its “Roche lobe” at periastron. The fundamental parameters fit well for masses of $\sim 13 M_{\odot}$ and $18 M_{\odot}$, respectively, although it is possible that the M star has lost a significant amount of its initial mass. This is near

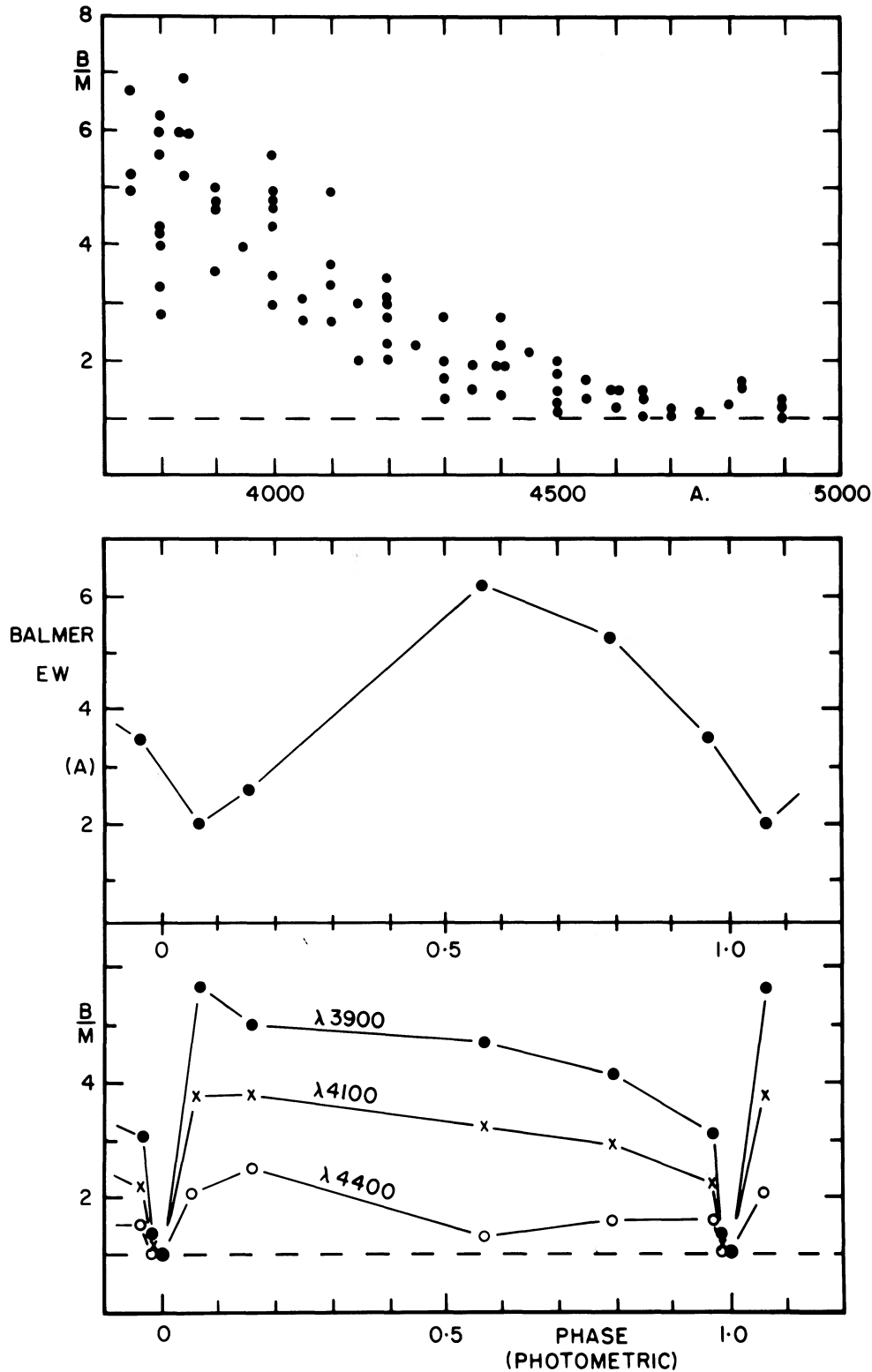


FIG. 6—(top) Ratio of B- to M-star intensity from all tracings derived by comparing of M-star line depths in and out of eclipse. (middle) Mean $H\gamma$, $H\delta$, and $H\epsilon$ equivalent widths with phase. Measurements were referred to the B-star continuum. (bottom) Ratio of B- to M-star continuum intensity with phase for three different wavelengths. Spectrophotometry is from Hale, KPNO, and DAO plates.

the upper limit of observed M-star masses.

In Table VII we list the few available masses for

cool supergiants. We also list the orbital period and eccentricity to give an idea of the scale of the system

TABLE IV

Parameters defined by $f(m) = 2.23$, $e = .55$, eclipse duration 100 days

$$\omega = 4^\circ, \phi_{\text{phot}}(\text{periastron}) = 0.08$$

$$(q = M_M/M_B)$$

	$q = 0.7$	$q = 1$	$q = 1.3$	$q = 1.4$	$q = 2.0$
Min. sep. (R_\odot)	1130	1330	1525	1600	2000
$R_{\text{crit}}(\text{polar}) (R_\odot)^*$	370	470	580	614	825
Trans.vel † (km/sec)	41	48	55	58	72
$i = 90^\circ$ R_M/R_\odot (eq)	350	400	460	480	600
R_M/R_\odot (pole)	334	380	440	455	570
R/R_{crit}^*	.90	.81	.76	.74	.69
R_B/R_\odot	36	42	48	50	62
$R=R_{\text{crit}}^*$ i	85.0°	82.6°	81.3°	81.0°	79.8°
R_B/R_\odot	32	34	36	37	43
M_M/M_\odot	5	9	16	19	42
M_B/M_\odot	7	9	12	13	21

B star $V \sin i \sim 300$ km/sec

* R_{crit} = radius of Roche limiting surface for given q and separation.

† relative velocity of the two components perpendicular to the observer's line of sight.

TABLE V

M Star Luminosities

Temp (K)	Radius (R_\odot)	M_{BOL}	$\frac{BC}{(mag)}$	M_V	$f(m)$	Mass H-R diag
2750 $^\circ$	614	-5.9	-3.4	-2.5	19	15
	825	-6.6	-3.4	-3.2	42	19
3000 $^\circ$	470	-5.6	-2.5	-3.1	9	13
	550	-6.2	-2.5	-3.7	16	17
	614	-6.3	-2.5	-3.8	19	18
	825	-7.0	-2.5	-4.5	42	22
3250 $^\circ$	614	-6.6	-1.7	-4.9	19	19

TABLE VI

Luminosity & Distance Estimates

$$A_V = 3E_{B-V} = 1.8 \text{ m.}$$

	M star	B star
m_V	9.5	11.3
m_B	11.6	11.6
M_{BOL}	- 6.5	- 5.3
BC	- 2.0	- 2.5
M_V	- 4.5	- 2.8
Dist. Mod.	12.2	12.3

and the changing amount of interaction. Some of this material has been compiled with the aid of the new catalog of spectroscopic binaries (Batten, Fletcher, and Mann 1977). It is interesting to note that all of these systems have fairly eccentric orbits. Although none of the masses are determined with much precision (because of observational difficulties similar to the ones encountered for AZ Cas), there seems to be no evidence for stars with masses greater than about $25 M_\odot$. Since we find hot supergiants with masses inferred from evolutionary tracts to be in excess of $60 M_\odot$, we conclude one or more of the following possibilities

may apply: (1) a large fraction of the mass of at least some of the cool supergiants has been lost during its evolution, or (2) the most massive stars evolve through this part of the H-R diagram so quickly that one would not expect to observe any in such a small sample of stars, or (3) stars with initial masses much greater than $\sim 20\text{--}30$ solar masses never reach this

TABLE VII
Masses of Late-type Supergiants

Star	Spectrum	P	e	$\frac{M_1}{M_2}$	Ref
31 Cyg	K4Ib+B4V	3784 ^d	.22	9.2	Wright & Huffman (1968)
32 Cyg	K5Iab+B4IV-V	1148	.30	~19	Wright (1970)
ζ Aur	K4II+B6V	972	.41	8.0	Lee and Wright (1960)
VV Cep	M2epIa+O9	7430	.35	19.8	Wright (1977)
KQ Pup	M2epIab+B	9752	.46	14-30?*	Cowley (1965)
α Sco	M2eIb+B4V	?very long visual binary	-	~25	diameter - Evans (1957) distance - Bertiau (1958)
AZ Cas	M0eIb+B0-1V	3404	.55	(~18)+	this study

*f(m) = 3.5, mass range is for $q = 1$ to 2

+f(m) = 2.2, mass given for estimated $q = 1.4$ and $i = 80^\circ$

cool part of the H-R diagram during their evolution (Chiosi et al. 1977). In addition, we know from the shape of the luminosity function that stars with $M > 30 M_\odot$ are less frequent than the lower mass stars. There are three other composite systems in the Galaxy similar to VV Cep and AZ Cas which are clearly more luminous: FR Scuti, W Cephei, and $-61^\circ 3575$. It would be extremely interesting to determine masses for one or more of these, as they might be expected to be at the upper mass limit for a cool supergiant.

We regard this study of AZ Cas as preliminary, since it leaves unanswered many important questions both with regard to the orbit and masses as well as the evolutionary state. Photometry and further spectroscopy both in and out of eclipse will give information on the period, possible apsidal motion, distortion of the M star, secular changes in both components, and the circumstellar shell of the B star. At present we have no satisfactory interpretation for the velocities of the M star excited lines in the blue region or the blue-shifted B-star Balmer lines, and we do not understand the apparent weakness of the interstellar K line.

We thank L. Margetish for assistance with some of the reductions. A.P.C. acknowledges support from the National Science Foundation, and thanks the DAO staff for their assistance and hospitality during her stay in Victoria. Dr. Ashbrook has kindly sent us his material on AZ Cas in advance of publication.

REFERENCES

- Ashbrook, J. 1956, *Harvard Ann.* Card No. 1340.
 ——— 1977 (private communication).
 Batten, A. H., Fletcher, J. M., and Mann, P. J. 1977, *Pub. Dominion Astrophys. Obs.* (in press).
 Bertiau, F. C. 1958, *Ap. J.* **128**, 533.
 Bidelman, W. P. 1969 (private communication).
 Chiosi, C., Nasi, E., and Sreenivasan, S. R. 1977 (preprint).
 Cowley, A. P. 1965, *Ap. J.* **142**, 299.
 ——— 1969, *Pub. A.S.P.* **81**, 297.
 Cowley, A. P., and Hutchings, J. B. 1977, *Inf. Bull. Var. Stars* No. 1318.
 Davis, D. 1947, *Ap. J.* **106**, 28.
 Evans, D. A. 1957, *Ap. J.* **62**, 83.
 Florkowski, D. R. 1975 (private communication).
 Herczeg, T. S., and Bonnell, J. T. 1976, presented at I.A.U. —Grenoble.
 Hiltner, W. A. 1956, *Ap. J. Suppl.* **2**, 389.
 Hutchings, J. B., and Redman, R. O. 1973, *M.N.R.A.S.* **163**, 209.
 Larsson-Leander, G. 1959, *Arkiv für Astr.* **2**, 347.
 Lee, E. K., and Wright, K. O. 1960, *Pub. Dominion Astrophys. Obs.* **11**, 339.
 Mendéz, R. H., Münch, G., and Sahade, J. 1975, *Pub. A.S.P.* **87**, 305.
 Peery, B. F. 1966, *Ap. J.* **144**, 672.
 Stothers, R. 1972, *Pub. A.S.P.* **84**, 373.
 Tempesti, P. 1975, *I.A.U. Circ.* No. 2825.
 Thackeray, A. D., and Hutchings, J. B. 1974, *M.N.R.A.S.* **167**, 319.
 Wawrukiewicz, A. S., and Lee, T. A. 1974, *Pub. A.S.P.* **86**, 51.
 Wright, K. O. 1970, *Vistas in Astr.* **12**, 147.
 ——— 1977, *J.R.A.S. Canada* **71**, 152.
 Wright, K. O., and Huffman, R. E. 1968, *Pub. Dominion Astrophys. Obs.* **13**, 275.